https://doi.org/10.5194/egusphere-2025-3163
Preprint. Discussion started: 15 August 2025

Spatial influence of agriculture residue burning and aerosols on land surface temperature

Akanksha Pandey[1], Richa Singh[1], Kumari Aditi[1,2], Neha Chhillar[1], Tirthankar Banerjee[1,2*]

[1] Institute of Environment and Sustainable Development, Banaras Hindu University, Varanasi, India.
[2]DST-Mahamana Centre of Excellence in Climate Change Research, Banaras Hindu University, Varanasi, India.
Correspondence to: T. Banerjee (tb.iesd@bhu.ac.in; tirthankaronline@gmail.com)

Abstract

The biophysical effect of agriculture-residue based fire through excessive release of energy and carbonaceous aerosols essentially unaccounted globally. Elucidating climate feedback from residue-based fire however, remain pertinent as energy released from fire pose potential to modify land surface temperature (LST) thereby, regional climate. Here, an observation-driven assessment of spatial change in LST due to concurrent release of energy and aerosols has been explored over northwest India using multiple satellite and reanalysis-based datasets. Initially, year-specific fire pixel density was computed to identify intensive fire zone encompassing only medium to large fire. Spatial analysis revealed positive correlation among FRP (fire radiative power), LST and AOD (aerosol optical depth) across the intensive fire zone. Residue-based fire accounted an increase in LST by 0.48°C and AOD by 0.19 yearly during peak fire season over intensive fire zone. A Random Forest non-linear model was used to regress potential influence of FRP and AOD on LST. Two pre-constructed scenarios were evaluated to ascertain FRP-AOD-LST nexus. Interestingly, both scenarios recognized FRP as a top predictor to influence LST followed by solar radiation and AOD. A significant enhancement in relative feature importance of FRP was also noted during days having high fire intensity and positive association against LST. Geographically Weighted Regression further explained spatial heterogeneity in LST modulation by FRP. Our analysis therefore, provides first evidence on crop residue-based fire on modifying regional climate by altering land surface temperature. It also underlines that extent of such perturbation is subject to year-specific fire intensity and govern by meteorology.

Keywords: Aerosols, Biomass burning, Fire, GWR, Random Forest.

https://doi.org/10.5194/egusphere-2025-3163
Preprint. Discussion started: 15 August 2025

Introduction

Burning agriculture residues is a widespread practice for quick removal of post-harvest crop leftover from the field over many parts of the world (Streets et al., 2003; Singh et al., 2018; Shyamsundar et al., 2019). While burning biomass is often associated with the practice of deforestation (Chuvieco et al., 2021), forest fire (van der Velde et al., 2021; Aditi et al., 2025) and shifting cultivation (Prasad et al., 2000); agriculture residue burning is more commonly associated with cleaning farmland, fertilizing soil, eradicating pests and weeds, and making land suitable for the subsequent crop (Graham et al., 2002; Korontzi et al., 2006; Lan et al., 2022). Agriculture residue burning is a common practice across the globe as reported in China (Streets et al., 2003; Zhang et al., 2020), South America (Graham et al., 2002), Southeast Asia (Lasko and Vadrevu, 2018; Yin, 2020) and from the northwest India (Singh et al., 2018, 2021; Sarkar et al., 2018). Crop residue burning over northwest India has been investigated widely from diverse perspectives. A widespread intensive burning during October to mid-November is a recurring phenomenon and often associated with poor air quality at downstream (Jethva et al., 2019; Singh et al., 2018), modifying aerosol loading and chemistry (Mhawish et al., 2022; Ravindra et al., 2023), influencing aerosol vertical stratification and radiative forcing (Hsu et al., 2003; Vinjamuri et al., 2020; Banerjee et al., 2021), inducing negative health impacts (Singh et al., 2021), and possibly shifting regional hydrological cycle (Kant et al., 2023). However, limited attention has been paid to investigate its effect on urban climate, especially on modulating lower atmospheric thermal budget which has been otherwise strongly evident in case of forest fire (Liu et al., 2018, 2019).

Across the northwest part of India, dual cropping pattern including rice and wheat crop is predominately practised over roughly 4.1 million ha of land. Such cropping pattern results in generating huge crop residues having poor nutrient content with high silica and ash fractions. Typically, residues from rice-wheat cropping system have limited economic value not being fitted as alternative fodder, biofuel or being procured in pulp and paper industries (Lan et al., 2022; Shyamsundar et al., 2019). Besides, with the advent of mechanical harvester in 1980s and enactment of groundwater preservation act in late 2000s, in situ indiscriminate burning of agriculture residues has been the recurrent choice of the local farmers to reduce the turn-around time between rice harvesting and subsequent sowing of wheat crop (Balwinder-Singh et al., 2019). India generates approximately 500 million metric tonnes (MT)

https://doi.org/10.5194/egusphere-2025-3163
Preprint. Discussion started: 15 August 2025

of crop residues per year with roughly 20-25% i.e. 100-120 MT/yr residues usually burn in the field itself, majority (~20-25 MT/yr) of such practised over northwest Gangetic plain (Lan et al., 2022; Balwinder-Singh et al., 2019). Unregulated burning of agriculture residues across the northwest part of India usually held responsible for approximately 300 Gg/yr of $PM_{2.5}$ and 50 Tg of CO_2 equivalent green-house gas emission (Singh et al., 2020). Interestingly, fire incidences have exhibited a consistent increasing trend with concurrent growth in vegetation index and aerosol loading (Vadrevu et al., 2018; Jethva et al., 2019). Beside emissions, biophysical effects of fire on surrounding ecosystem could be many as fire drives several consequential changes, be it in modifying surface energy balance, redistributing nutrients and species, modifying surface albedo thereby, altering evapotranspiration rate (Ward et al., 2012; Liu et al., 2019). Additionally, fire could also induce certain biogeochemical and biophysical stresses on local environment by modifying atmospheric composition and surface properties (Andela et al., 2017; Aditi et al., 2025). Such transformation in the native landscape coupled with excessive release of energy, emission of aerosols and its precursors may therefore, have several potential implications on the local environment.

Majority of the researches involving biomass-based fire are dedicated to recognize land and atmospheric processes and precursors on initiating and propagating fire, quantifying emissions and evaluating land surface-atmosphere exchange. There is however, limited understanding on how biomass-based fire induce climate feedback by altering Earth's surface radiative budget and land surface temperature (Bowman et al., 2009; Andela et al., 2017). Plausible explanation to this includes limited observation and associated uncertainties in estimating key biophysical processes like surface albedo, land-atmosphere exchange of sensible heat flux and water vapor, changes in evapotranspiration rate during pre- and post-fire events. There are instances when global forest fire incidences and size have been linked with modifications in land surface temperature (LST; Alkama and Cescatti, 2016; Liu et al., 2018, 2019). Likewise, Liu et al. (2019) noted an enhance in mean annual LST over burned forest area in the northern high latitudes. Similar evidence of increase in summertime surface radiometric temperature over temperate and boreal forests in the Northern Hemisphere was accounted by Zhao et al. (2024). Alkama and Cascatti (2016) evident a corresponding increase in mean and maximum air temperature over the arid zone due to loss of forest cover. However, fire induced thermal forcing was reported to be constrained by fire size (Zhao et al.,

https://doi.org/10.5194/egusphere-2025-3163
Preprint. Discussion started: 15 August 2025

2024) and often, relatively small scale burning, particularly involving crop residues on agriculture farmland may not be sufficient enough to induce robust change in surface albedo and evapotranspiration, resulting insignificant variation in LST. Incidence of elevated LST over different provinces in China due to agriculture residue burning has only recently reported by Zhang *et al*. (2020). A spatially inconsistent increase in LST correlated well with fire count, having highest LST gradient noted in 4 to 10 km distance from the central point of cop residue burning and remained valid till 1-3 days. In contrast, post-harvest fire incidence over northwest India has not yet explored in terms of its effect on LST. This induces significant uncertainty in recognizing climate feedback of crop residue burning and warrants a better understanding of the underlying mechanism.

This study aims to explore immediate biophysical effect of agriculture crop residue fire on surface temperature over northwest India. By integrating spatially and temporally consistent satellite- and reanalysis- based observations on fire counts, fire radiative power, land surface temperature, aerosol loading and regional meteorology over intensive fire zone, we tried to establish time-bound changes in LST with concurrent variations in fire strength. Several statistical means were explored to construct the changes in LST with fire severity. A space-for-time approach was used to construct changes in LST and AOD due to recurrent changes in FRP over the fire season. Specifically, we tried to investigate two questions, (1) does land surface temperature respond to changes in fire intensity over northwest India, and (2) how local meteorology and aerosol loading modulate LST variation with respect to space and time? To best of our knowledge, such understanding on fire regulated changes in LST has not yet explored over northern India and could provide vital evidence on climate feedback from crop-residue based fire.

2. Dataset and methodology

2.1 Study domain

Post-harvest burning of biomass is mainly practised over the northwest part of the Indo-Gangetic Plain (IGP) of South Asia. The region encompassing the agrarian states of Punjab and Haryana is particularly productive and accounts for a whopping 60-70% of India's food grain generation. Coupled with increased production of rice and wheat crop, generation of crop residues has been increased multi-fold in recent years resulting higher intensity in crop-based fire over the region (Jethva et al., 2019). For this research, the geospatial analysis

https://doi.org/10.5194/egusphere-2025-3163
Preprint. Discussion started: 15 August 2025

of LST in continuation with fire activity and aerosol loading has been made over the northwest part of India for the months of October to November between year 2017 and 2021. The combination of high agricultural output, extensive biomass burning, and documented increases in fire activity renders this region specifically appropriate for analysing fire dynamics and their environmental consequences. However, instead of pre-identifying a fixed research domain, we have retrieved year-wise fire signal across the northwest India constrained by crop land. This led to the selection of core-study region differs annually with respect to year-specific fire intensity and spatial trend (as in Fig. S1, in supplementary file), but all eventually bound to 29.2770° to 32.1625° N and 73.8996° to 77.0718° E, as illustrated in Fig. 1b.

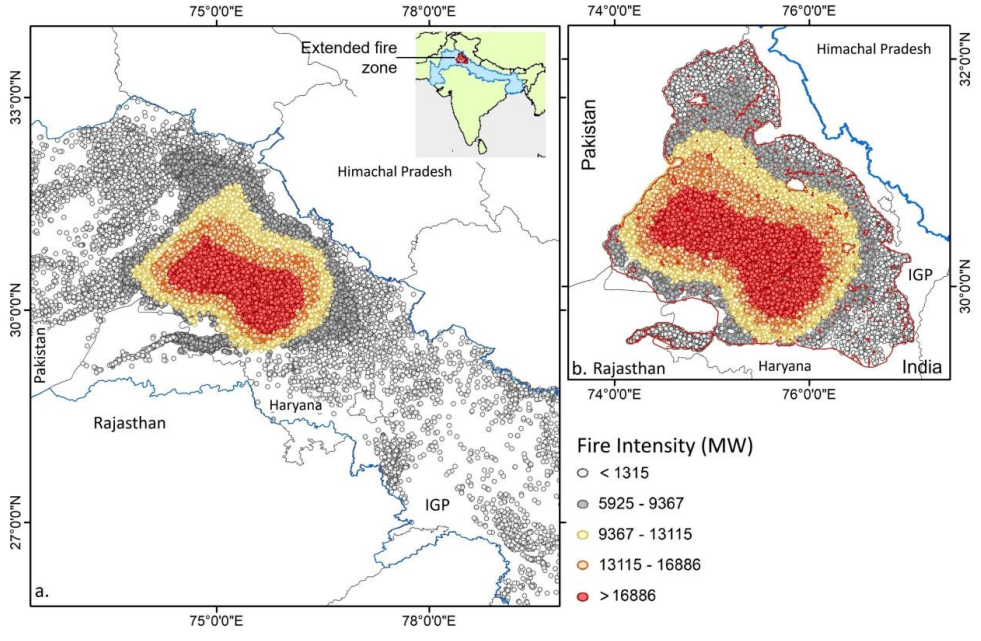

Fig. 1. Spatial variation in satellite-based fire radiative power across northwest India, distribution of FRP-based fire intensity (MW/pixel) (a) and domain selected for retrieval and processing of SNPP VIIRS FRP, AOD and Aqua MODIS LST (b).

NOTE. The region marked with blue in Fig. 1a subset indicates the Indo-Gangetic Plain (IGP) spanning from Pakistan to Bangladesh through India. The extended fire zone selected for analysis is marked with red within the IGP and has been shown in detail in Fig. 1a with fire pixel density. The selection criteria of the spatial domain are discussed in section 2.3. The pixel size of VIIRS VNP14IMG is 375x375 m^2. India shape file is acquired from Survey of India archive.

https://doi.org/10.5194/egusphere-2025-3163
Preprint. Discussion started: 15 August 2025

2.2 Spatial dataset

Active fire count data was retrieved from the standard fire product of Visible Infrared Imaging Radiometer Suite (VIIRS) Collection-2 Level-1B (VNP14IMG) available at 6-min L2 swath at 375 m resolution. The VIIRS onboard the Suomi National Polar-orbiting Partnership (SNPP) satellite is a cross-track single-angle scanning radiometer which was launched in year 2011 under joint operation of NASA and NOAA. The VIIRS fire detection algorithm typically extends well refined and validated MODIS Fire and Thermal Anomalies product (Giglio et al., 2003). The I-band based fire detection algorithm primarily utilizes brightness temperature of Channel I4 on middle infrared spanning from 3.55 to 3.93 µm, centred at 3.74 µm. Additionally, to isolate the active fire spots from the fire-free background channel, a single gain I5 at thermal infrared regions (10.5–12.4 µm) is also considered. Rest of the I-band channels i.e. I1 to I3, covering visible, near and short-wave IR are used to distinguish pixels with cloud, water and sun-glint (Schroeder et al., 2014). The VIIRS fire database was considered due to its superior precision and accuracy in identifying relatively small fire, greater spatial resolution at footprint and pixel saturation temperature (Vadrevu et al., 2018; Li et al., 2018; Aditi et al., 2023). For this experiment, SNPP VIIRS 375 m C2 L1B active fire count data with nominal (fire mask class 8) and high confidence (fire mask class 9), was retrieved over northwest India from year 2017 to 2021 (all inclusive).

Fire radiative power (FRP) quantifies the release of radiative energy from biomass burning integrated at all angles and wavelengths over a spatial scale. Measured in Watt, FRP retrieval quantifies the release of heat energy against time and in many instances linearly associated with the rate of fuel consumption and emission (Ichoku et al., 2008; Nguyen and Wooster, 2020). A detailed description on FRP retrieval and comparison among the sensors are available in Wooster et al. (2003, 2005) and Ichoku et al. (2008). Li et al. (2018) concluded VIIRS FRP as comparable with MODIS FRP in most of fire clusters and very stable across swath. Here, FRP (MW) was processed from the SNPP VIIRS C2 Level-2 (L2) 375 m active fire product (VNP14IMG). VIIRS FRP was used as a proxy of fire intensity and potential emission strength from the biomass burning area, and considered as a direct measurement of radiative energy being released from individual fire pixel.

Land surface radiometric temperature (LST) at 1 km spatial resolution was utilized from Moderate Resolution Imaging Spectroradiometer (MODIS) version 6.1 Land Surface

https://doi.org/10.5194/egusphere-2025-3163
Preprint. Discussion started: 15 August 2025

Temperature and Emissivity retrievals product (MYD11A1). Typically, LST indicates thermodynamic temperature of the interface atmospheric layer within soil, plant cover and lower atmosphere, and serves as an indicator of land-atmosphere interaction and exchange (Li et al., 2023). Here, MODIS MYD11A1 radiometric dataset with quality flag '00' was specifically chosen considering its broad swath and wider applicability in estimating land surface temperature. Besides, MODIS LST is validated against ground observations on diverse land covers and reported to provide realistic estimate of surface temperature (Wan, 2014) with a uncertainty of ≤0.5 K. Both daytime maximum and nighttime minimum LST approximately at 1:30 PM and 1:30 AM local time respectively, are available. However, to better approximate the timing of VIIRS fire count retrieval at 1:30 PM local time when crop residue-based fire presumably remains at peak, surface retrievals of LST was only made from MODIS onboard Aqua satellite.

Aerosol optical depth (AOD) from Visible Infrared Imaging Radiometer Suite (VIIRS) sensor on-board SNPP satellite offers accurate estimation of columnar aerosol loading at 550 nm over land. Accuracy of VIIRS V1 DB AOD was evaluated extensively over South Asia by Aditi et al. (2023) and reported to provide stable AOD retrieval against AERONET. Sayer et al. (2019) reported an estimated error of ±(0.05+20%) in VIIRS AOD dataset. Here, Deep Blue (DB) Version 1 AOD dataset (AERDB_L2_VIIRS_SNPP Level-2) was used to retrieve AOD with a nominal spatial resolution of 6 km at nadir. Only quality assured AOD (QA ≥ 2) was retrieved for the months of October to November for years 2017 to 2021 over selected spatial domain.

Terra/Aqua MODIS land cover data was used to discriminate crop land against the rest to filter out thermal anomalies exclusively over the agriculture land. To achieve this, MODIS L3 V6.1 Global Land Cover type product (MCD12Q1) was retrieved from LAADS DAAC site for year 2017, available at 0.5 km spatial resolution. MODIS land cover types adopts International Geosphere-Biosphere Programme (IGBP) and other land type classification schemes to classify land cover. Here, land cover type 12 (cropland) was earmarked to isolate the agriculture land from its surrounding (Fig. S2).

Lower surface meteorological data including air temperature (At), total solar radiation flux (Sr), precipitation (Pr) and relative humidity (RH) was procured from European Centre for Medium-Range Weather Forecasts (ECMWF) AgERA5 dataset. The AgERA5 dataset has been generated by Copernicus Climate Change Service (2020) from hourly ECMWF ERA5 dataset for

https://doi.org/10.5194/egusphere-2025-3163
Preprint. Discussion started: 15 August 2025

specific agro-ecological based applications. The meteorological data were pre-customized with temporal aggregation aligned to local time zones and spatial enhancement to a 0.1° resolution using grid-based variable-specific regression model. Here, air temperature at 2 meters above the surface, total solar radiation flux received at the surface over a 24-hour time period, and relative humidity at 2 meter height was selectively used over pre-identified intensive crop-based fire zone.

2.3 Spatial analysis for fire-aerosols-LST association

2.3.1 Selection of intensive fire zone

Post-harvest specific crop residue burning typically commences during mid-October and reaches its peak intensity during mid-November, particularly over northwest India. All the spatial analysis was therefore, conducted for the months of October and November for year 2017 to 2021 (all inclusive). The VIIRS 375 m fire product was able to retrieve active fire pixels across the IGP with marked spatial heterogeneity. To ascertain a representative region having predominance of residue-based fire, spatial comparison of fire pixel density was made using daily retrieved VIIRS FRP dataset. The selection of FRP over fire count as a criterion to isolate intensive fire region was driven by the fact that FRP directly relates energy release from active fire thereby, potentially modulate the spatial change in LST. Pixel density of fire radiative power was assessed at 1.5 x 1.5 km grid to compare spatial variations in FRP intensity across northwest India. To compute FRP density, a ratio between FRP and the grid area was computed following the protocol mentioned in Giglio et al. (2006).

Initially, geospatial variations in fire intensity and associated changes in LST and AOD was assessed. Spatial intercomparison between fire intensity with LST and AOD was made over the designated zone shown in Fig. 2a. The zone was earmarked to cover an extended geographical area without imposing any discrimination between low and high FRP density over the northwest India. The zone was henceforth, referred as '*extended geographical region'* as it combines fire intensity across the years and was solely meant to constitute spatial association between the dependent and predictor variables.

https://doi.org/10.5194/egusphere-2025-3163
Preprint. Discussion started: 15 August 2025

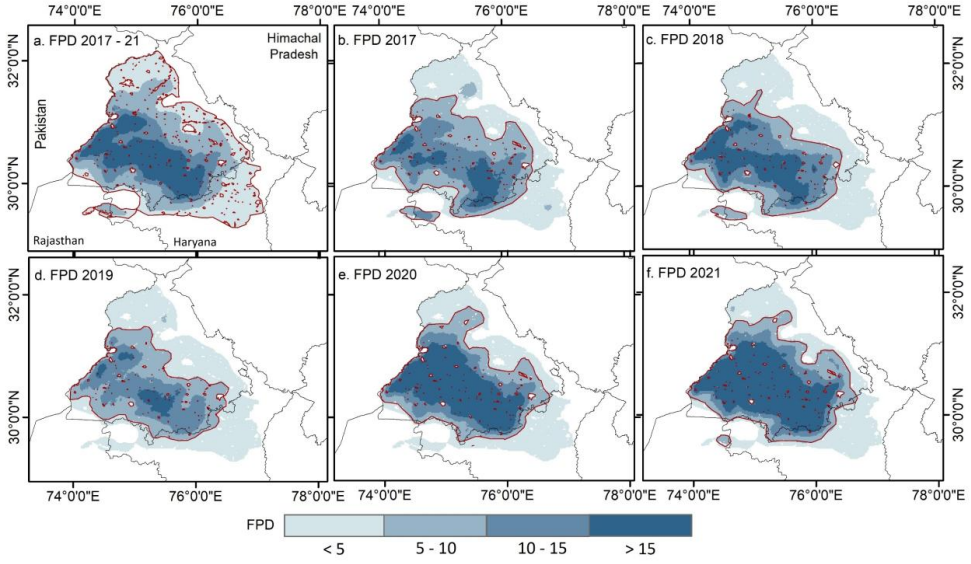

Fig. 2. Selection of high intensity residue-based fire zone based on fire radiative power pixel density (MW 2.25 Km^{-2} day^{-1}).

NOTE. Fig. 2a indicates the 'extended region' demarcating the entire area with varying fire intensity selected for spatial analysis. Rest of the figures classify year-specific 'intensive fire zone' used to retrieve all the variables for spatiotemporal analysis.

In contrast, to establish potential effect of day to day variations in fire intensity and aerosol loading on LST, comparatively high intensity fire zone was designated against low intensity zone. To achieve this, entire crop-residue burning region of northwest India was earmarked constraining low (<5 MW $grid^{-1}$) to high FRP density (>15 MW $grid^{-1}$). Spatial variations in FRP density were compared among the selected years and region(s) was identified considering a threshold FRP density >5 MW $grid^{-1}$ area (Fig. 2b-f). This ensured a better representation of the effect of medium to large crop-based fire on regional LST as very small-intensity fire deem to extinguish faster while being inconducive to considerably influence surface temperature (Zhao et al., 2024). All the spatial datasets were subsequently retrieved exclusively within the year-wise designated '*intensive fire zone*' having FRP density >5 MW $grid^{-1}$, and included for ascertaining FRP-AOD-LST association. Incidentally, area having high FRP density (>5 MW $grid^{-1}$) remained almost consistent as illustrated in Fig. 2(b-f) and quantified in Table S1. It is noteworthy, the fire intensive region was pre-filtered based on the

https://doi.org/10.5194/egusphere-2025-3163
Preprint. Discussion started: 15 August 2025

Terra/Aqua MODIS land cover data to deselect any FRP pixel that emerged from a non-agricultural/crop land.

2.3.2 Selection of temporal window

As the region with higher fire pixel density was isolated, our subsequent effort was to identify temporal window to assess potential association between fire intensity and other explanatory variables on the identified zone. Selection of temporal window for spatial analysis was based on two scenarios as illustrated in Fig. 3. Scenario (1) was to quantify the influence of FRP, aerosols and other parameters on LST when fire intensity starts to build up and remain persistent over the intensive fire zone. Scenario (1) therefore, considers the day as initiation when FRP starts to build up for the first time in October and consistently exceeds 1500 MW with a corresponding 50% increase in area weighted FRP aggregate against its previous day. The Scenario (1) concludes with the same approximation during November with a 50% decline in aggregate FRP compared to its previous day. The dates selected for scenario (1) are shown in Table S2 with two exceptions. First, in year 2018 when a >50% criteria was not met despite having an aggregate FRP >1500 MW and second, in year 2017 when a prior decrease (>50%) in FRP was avoided because of subsequent rise in fire intensity.

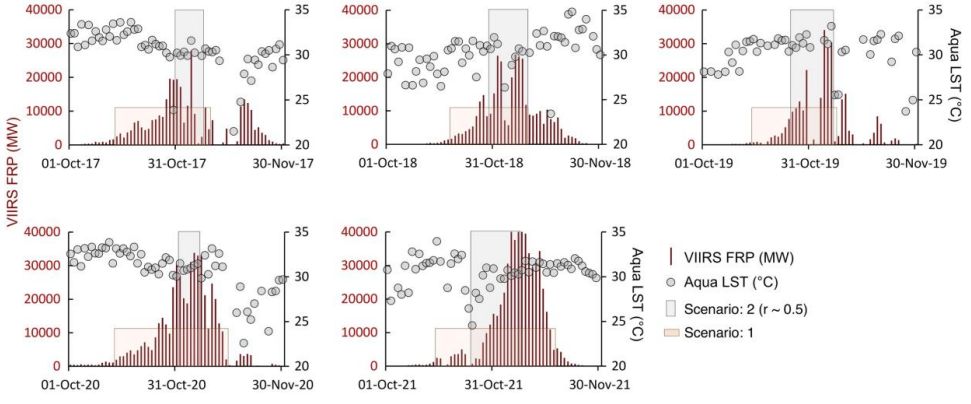

Fig. 3. FRP time series against LST over year-specific intensive fire zone with marked time frame for both scenarios selected for geospatial modelling.

NOTE. All the spatial datasets including FRP, fire count, AOD and LST were retrieved exclusively within the year-wise designated fire intensive zone having FRP density >5 MW grid^{-1}. Scenario (1) refers extended timeframe to consider entire fire period while scenario (2) select the interlude having high temporal coefficient between FRP and LST.

https://doi.org/10.5194/egusphere-2025-3163
Preprint. Discussion started: 15 August 2025

To constitute scenario (2), statistical association between day-specific aggregate FRP and spatially average LST retrievals were examined. Precisely, pixel-based LST was averaged over intensive fire zone and compared against area weighted FRP sum on day-to-day basis. Here, a temporal window ('*Scenario: 2*' in Fig. 3) for spatial analysis was identified fulfilling two criteria; first, the end date of the window should coincide with the day having relatively high FRP and second, the selected window should achieve a robust and positive correlation ($r \geq 0.5$) between FRP and LST. Such restricted criteria were put to ensure that we only select year-specific window(s) when FRP (so the fire count) increases with time and exhibit a strong association with regional LST. It is noteworthy that selecting multiple windows within a year having coinciding days was avoided while ensuring windows should not contain more than 5% of missing days, irrespective of parameters.

2.4 Spatial correlation between fire, aerosols and LST

To identify spatial association between FRP, LST and AOD over the crop residue-based fire zone, pixel-based spatial correlation coefficient was computed and its statistical significance ($P<0.05$) was tested across the study domain. This enables us to identify region having robust co-variability across the thermal conditions with varying fire intensity and columnar aerosol loading.

2.5 Hurst Exponent

The Hurst exponent is a statistical measure used to characterize the properties of a time series without imposing assumptions regarding its statistical distribution. Originally introduced by H.E. Hurst (1951) in the context of hydrological studies and later refined by Markonis and Koutsoyiannis (2016), it has since been widely applied across diverse scientific disciplines for analysing long-term trends and variability. Here, Hurst exponent was computed for FRP, AOD and LST timeseries to recognize long term persistence of the dataset. The main calculation procedures were as follows (Granero et al., 2008):

A time series x(t) is given,

$$(\mathrm{x})_{\mathrm{t}} = 1/\tau \sum_{t=1}^{\tau} x(t) \quad t = 1, 2, 3 \ldots \tag{1}$$

The cumulative deviation is determined using Eq. 2:

$$X(t, \tau) = \sum_{u=1}^{\tau} (x(u) - (\mathrm{x})_{\mathrm{t}}), \text{ with a condition of } 1 \leq \mathrm{t} \leq \tau. \tag{2}$$

https://doi.org/10.5194/egusphere-2025-3163
Preprint. Discussion started: 15 August 2025

Extreme deviation sequence, is defined as:

$$R(\tau) = \max_{1\le t\le \tau} X(t,\tau) - \min_{1\le t\le \tau} X(t,\tau) \quad where\ \tau = 1, 2, 3 \ldots \tag{3}$$

The standard deviation sequence is calculated by Eq. (4):

$$S(\tau) = [1/\tau \sum_{t=1}^{\tau} (x(t) - (X)_\tau)^2]^{1/2} \quad where\ \tau = 1, 2, 3 \ldots \tag{4}$$

By considering both extreme deviation sequence and standard deviation sequence,

$$R/S = R(\tau)/S(\tau) \text{ when assuming } (R/S) \propto (\tau/2)^H \tag{5}$$

Hurst exponent varies between 0 and 1. A value of 0.5 signifies that the time series behaves as a stochastic process lacking persistence, indicating that future trends in the series are independent of those observed during the study period. Values exceeding 0.5 denote persistence in the time series, reflecting a tendency for future changes to follow the same trend as in the past; higher values correspond to stronger persistence. Values below 0.5 indicate anti-persistence, meaning the time series exhibits a tendency to reverse its trend over time, with lower values indicating stronger anti-persistence (Peng et al., 2011).

2.6 Space-for-time approach

A space-for-time approach (Liu et al., 2019) was used to assess and compare heterogeneity in AOD and LST against the variation in FRP within residue-based fire zone. Initially, year specific intensive fire zone was categorically divided in to multiples of 10x10 km^2 grid cell, selected on the basis of resolution of VIIRS AOD. Daily LST, AOD and FRP was subsequently retrieved over individual grid for the duration selected under scenario two when both fire and corresponding LST increases with time. After filtering out the grid cell having missing values for either LST or AOD, grids were classified into groups, one, having zero FRP (no fire) against all the grids having FRP > 0, indicating presence of fire. Subsequently, LST and AOD across all the grids with zero FRP were averaged ($LST_{no\ fire}$) and compared against mean LST (LST_{fire}) computed by averaging the grids exhibiting residue-based fire. A positive (negative) ΔLST ($LST_{fire} - LST_{no\ fire}$) indicates a warming (cooling) induced by fire and was used to assess change in LST due to residue-based fire for the selected years. A similar approach was also used to constitute AOD variations utilizing grid-based retrievals.

https://doi.org/10.5194/egusphere-2025-3163
Preprint. Discussion started: 15 August 2025

2.7 Multicollinearity assessment

Multicollinearity, where independent variables are highly correlated, can distort regression model estimates and obscure the true relationships between predictors and the target variable (Graham, 2003). In this study, multicollinearity was assessed by calculating the Variance Inflation Factor (VIF) using the statsmodels library. A VIF value of 1 indicates no multicollinearity, values between 1 and 5 suggest moderate correlation, and values above 5 indicate significant multicollinearity (Daoud, 2017).

2.8 Random Forest regression

Random Forest (RF) regression was used to model the relationship between the dependent (LST) and the predictor variables (AOD, At, RH, Sr, Pr, FRP). It is noteworthy that RF was employed on daily-based spatial average of individual dataset to model the change. The RF is a non-linear ensemble learning method that constructs multiple decision trees using bootstrapped samples of the training data, with random subsets of predictors considered at each split. The final prediction is obtained by averaging the outputs of all trees, which improves generalization and mitigates overfitting. Due to its ability to model complex non-linear relationships and handle multicollinearity and interactions among predictors effectively, RF is particularly suited for environmental modelling tasks (Breiman, 2001; Puissant et al., 2014).

The RF model was implemented using Scikit-learn's RandomForestRegressor with 100 trees and a fixed random seed to ensure reproducibility. A correlation pattern of prime predictor with dependent variable was also plotted through partial dependence plots (PDPs). The dataset was partitioned into training (75%) and testing (25%) subsets, and model performance was assessed using statistical metrics like coefficient of determination (R^2), Root Mean Squared Error (RMSE), and Mean Absolute Error (MAE), allowing a comprehensive evaluation of model accuracy and prediction error.

2.9 Assessment of relative feature importance

Variable importance was computed from the trained RF model using the mean decrease in impurity approach, which quantifies the relative contribution of each predictor variable in reducing variance in the model's prediction. This analysis offers a focused understanding of the dominant variables driving spatial and temporal variability in LST.

https://doi.org/10.5194/egusphere-2025-3163
Preprint. Discussion started: 15 August 2025

Feature importance were extracted and ranked to identify the most influential predictors of LST during diverse fire intensity scenarios. To facilitate meaningful comparison across predictors, the relative contribution of each feature was calculated as the ratio of its importance score to the sum of all feature importances. This normalized metric reflects the proportional influence of each predictor within the model. Since Scikit-learn's RandomForestRegressor.feature_importances_ provides these values as normalized contribution summing to 1, the output inherently aligns with the relative contribution.

2.10 Spatial heterogeneity assessment using GWR

Spatial heterogeneity in FRP modulated variations in LST across intensive fire zone was further assessed using Geographically Weighted Regression (GWR). It is an advanced statistical method designed to capture heterogeneity in association across space between predictors and dependent variables by constraining spatially-varying coefficient estimates (Brunsdon et al., 1996). The GWR allows regression coefficients to vary locally across geographic space and effectively track these coefficients by using a weight matrix which evaluates the association between kernel and nearby samples (Yang et al., 2020). Unlike global models that assume spatial stationarity, GWR estimates location-specific parameters, thus providing a nuanced understanding of spatially varying relationships between dependent and independent variables (Fotheringham et al., 2009). The GWR model is formally expressed as:

$$yi = \beta_0(ui, vi) + \sum_{k=i}^{m} \beta k(ui, vi)\, xik + \varepsilon i \quad (6)$$

where (ui, vi) are the coordinates of observation i, βk(ui, vi) are spatially varying coefficients, xik are predictor variables, and εi denotes random error. Here, local parameter is estimated using a weighted least square in which each observation is weighted according to its spatial proximity to the location being evaluated. The weights are determined by a spatial kernel function and a bandwidth parameter, which controls the degree of spatial influence. Choosing an optimal bandwidth is therefore, critical to balance the trade-off between model bias and variance. In this study, the optimal bandwidth is selected through an iterative optimization process that minimizes the corrected Akaike Information Criterion (Fotheringham et al., 2009). This also ensures robust estimation of local relationships while accounting spatial non-stationarity in the dataset.

https://doi.org/10.5194/egusphere-2025-3163
Preprint. Discussion started: 15 August 2025

3. Results and discussions

3.1 Spatial association between fire, aerosols and LST

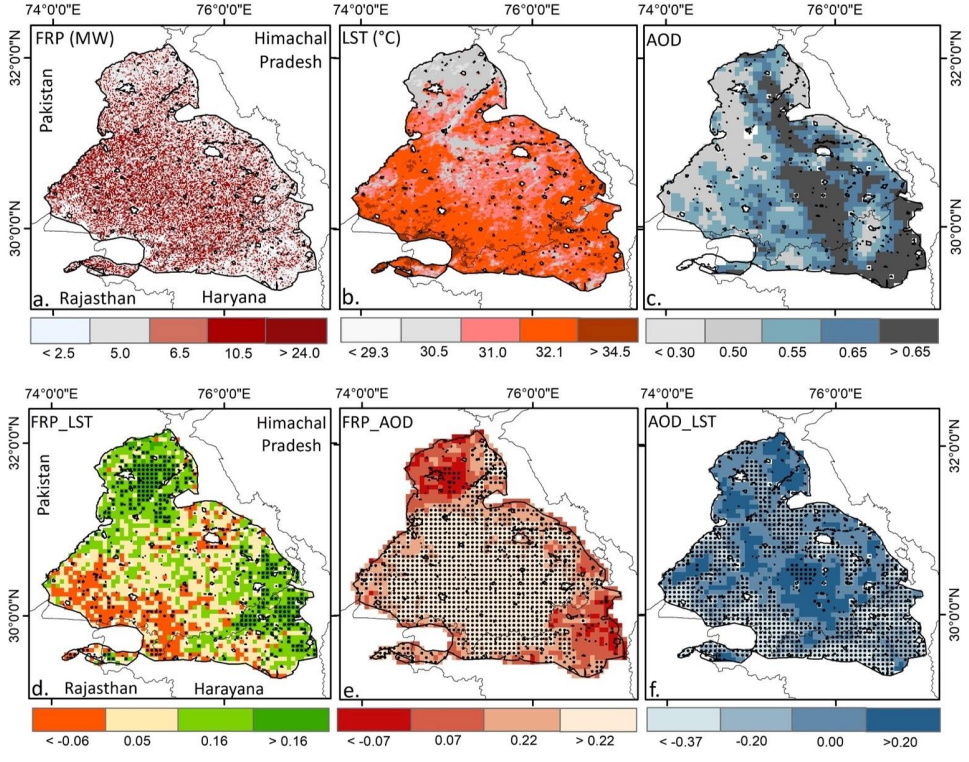

Fig. 4. Spatial association between predictor (FRP, AOD) and dependent variables (LST), 5-year mean FRP (a), LST (b) and AOD (c), and spatial correlation between FRP_LST (d), FRP_AOD (e) and AOD_LST (f) over extended geographical region.

NOTE. To constitute a spatial association, daily retrievals of FRP, AOD and LST pixels were converted to a common 6x6 km grid. Spatial correlation between FRP, LST and AOD daily retrievals on selected grid was made for the entire duration over extended geographical region. Significant correlation (P<0.05) is shown with black dot.

Spatial variations in FRP, LST and AOD averaged during October to November between 2017 and 2021 over extended geographical region without discriminating low to high fire intensity is shown in Figure 4(a-c). Variations in FRP did not reveal any specific spatial pattern while temporal differences were robust with approximately 100% increase in monthly mean FRP in the month of November (310,188 MW month^{-1}) compared to October month (152,616 MW month^{-1}, Table S3). Spatial pattern in LST however, indicate a marked heterogeneity with comparably high temperature at lower southern region that declined gradually towards

https://doi.org/10.5194/egusphere-2025-3163
Preprint. Discussion started: 15 August 2025

north. This could potentially due to the proximity of mountainous region which partially offset the fire induced elevated LST in the northern part. Overall, spatially averaged LST monthly mean varied from 28 to 32 °C with slightly higher temperature during October (31.0±1.6 °C) compared to November month (29.0±2.4 °C). On the contrary, a spatially robust signature in columnar aerosol loading was apparent across the extended geographical region. Comparatively high AOD (>0.65) was retrieved at the centre that too receded towards its border (<0.30). Such spatially robust variation in columnar aerosols potentially influenced by the varying intensities of fire associated emission of aerosols and trace gas precursors. A strong deviation in monthly mean AOD (October: 0.59 ±0.08; November: 0.82±0.12) was also accounted which either influenced by November specific increase in fire intensity and/or meteorological variables, especially due to the decline in planetary boundary layer height (Banerjee et al., 2022).

Spatial association between VIIRS FRP against MODIS LST and VIIRS driven AOD daily retrieval was also assessed over pre-identified geographical region (Fig. 4d-f). Spatial correlation between pixel-based FRP against LST reveals a heterogenous positive association over major portion of the area except southern part. A statistically significant association ($P<0.05$) between FRP and LST indicates potential influence of crop-based fire on surface temperature. FRP and AOD also accounts a statistically significant association across the central part where fire intensity was considerably high compared to its outskirts. Such spatial covariation between fire intensity and columnar aerosol loading reemphasize the possible influence of incremental aerosols and its precursors' emission from biomass burning on columnar aerosols. Biomass burning aerosols primarily being carbonaceous smoke particles are reported to modulate lower atmospheric thermal budget (Bond et al., 2013). Spatial association between AOD and LST provide further evidence on possible fire-aerosols-surface temperature nexus over northwest India. A comparatively low but significant positive association between AOD and LST was possibly the consequence of smoke aerosols induced lower atmospheric warming, as was also accounted by Gomez et al. (2024) over western United States during 2017 California wildfire.

3.2 Evaluation of Hurst exponent

Hurst exponent was evaluated to ascertain long-term persistence of fire intensity, surface temperature and aerosol loading time-series over the intensive fire zone. Principally,

https://doi.org/10.5194/egusphere-2025-3163
Preprint. Discussion started: 15 August 2025

Hurst exponent is employed to quantitative segregate a stochastic time series (H: 0.50) against a sustainable (H> 0.50) and anti-persistence time-series (H< 0.50) of pixel-based FRP, LST and AOD following the protocol as mentioned in Markonis and Koutsoyiannis (2016) and Chen et al. (2022).

It could be seen from Fig. 5 that almost entire extended region over northwest India appears to have a Hurst exponent >0.50 for FRP with relatively high exponent (0.60-0.70) at the centre. Although the variations in Hurst exponent was not highly consistent as fire intensity fluctuates with time and space, we note that the accounted FRP time-series over major proportion of the region should sustain in longer time period. Similarly, a high exponent for LST (>0.50) across the region entails LST time-series too persisted and possibly remain stable in near future. For agriculture land located at the northern part, Hurst exponent appeared to be >0.65 indicating a strong trend in LST time series. For regional aerosol loading, barring few isolated tiny patches, Hurst exponent enhanced with space and time and accounted highest value (>0.75) over the central part. The region also coincides with area having high AOD (>0.65) and statistically significant association for FRP and AOD.

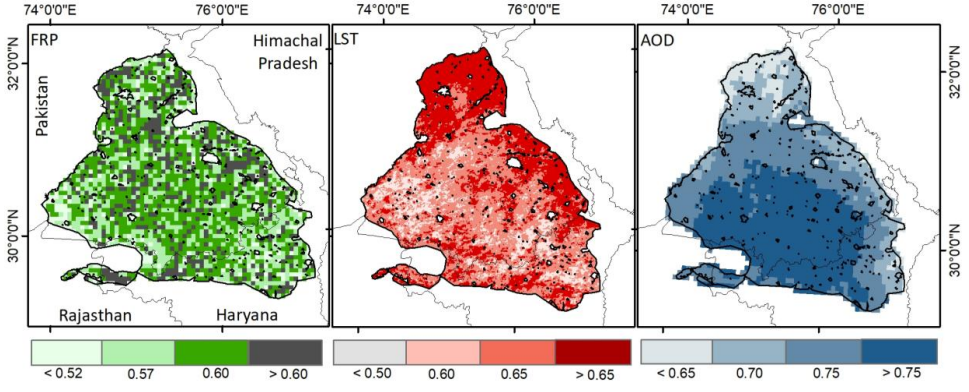

Fig. 5. Estimating FRP, LST and AOD time-series persistence in extended geographical region .

Its noteworthy that we have avoided analysing trend in respective time series as such estimation was not within the scope of the present research. Besides, a 5-year time period may not result statistically robust trend deemed comparable with previous estimates. Long-term trend in fire dynamics and aerosol loading over the northwest region has however been reported by several researches, like Vadrevu and Lasko (2018), Jethva et al. (2019) and Singh et al. (2020).

https://doi.org/10.5194/egusphere-2025-3163
Preprint. Discussion started: 15 August 2025

3.3 Surface temperature and aerosols response to fire intensity

Fire intensity in terms of pixel-based FRP, aerosol loading and surface temperature were retrieved to constitute respective daily means and spatial mean based on five year retrievals. It is noteworthy that to account immediate response of fire intensity and aerosol loading on surface temperature, all variables were retrieved exclusively over year wise intensive fire zone having cumulative FRP ≥ 5 MW grid^{-1} as illustrated in Fig. 2(b-f).

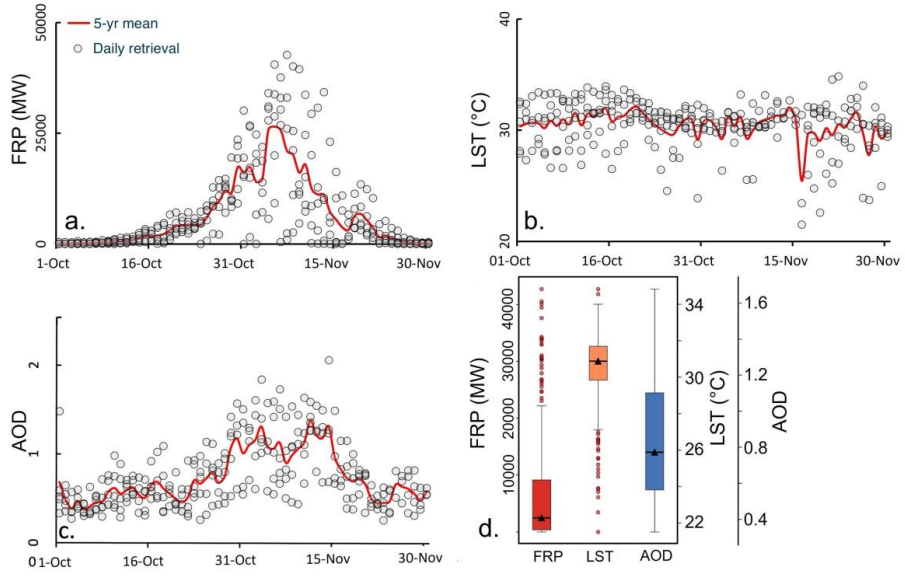

Fig. 6. Time series of five-year mean fire radiative power (FRP, a), land surface temperature (LST, b) and aerosol optical depth (AOD, c) against daily retrievals, (d) covariation of FRP, AOD and LST over intensive fire zone.

NOTE: Gray dots indicate daily retrievals from October to November over the years from 2017 to 2021 while 5-yr mean is the daily average based on retrievals from 2017 to 2021, and is indicated with red line.

A robust temporal pattern could be extracted from FRP timeseries (Fig. 6a) which reciprocates well with corresponding daily variations in fire count (Fig. S3). We note FRP initiates during mid-October over northwest India and reaches its peak consistently in the first week of November before reducing mid-November onwards. In contrast, temporal pattern in five-year mean LST timeseries is less intensive as daily retrievals shows extensive range of deviations. Regional LST clearly reflects both inter- and intraannual fluctuations, as shown in

https://doi.org/10.5194/egusphere-2025-3163
Preprint. Discussion started: 15 August 2025

Fig. S4. FRP time series however, matches well with mean columnar aerosol loading emphasizing possible effect of emission of aerosols and its precursors from extensive biomass burning. The characteristic rise in AOD during first two weeks of November possibly exhibits the direct response to elevated fire intensity as columnar aerosols consistently surpass 1.00 over the intensive fire zone. Interestingly, every year in between October 25 to November 20, 90% of daily-AOD exceeds 5-yr mean AOD (0.74±0.28) with corresponding 800% rise in average FRP (13085±6825 MW) compared to rest of the period (1148±1478 MW). Dring this interlude, five-year mean columnar AOD corelates well with 5-yr aggregate FRP (r: 0.46) and mean LST (0.41) which was otherwise, not the case for the remaining period (AOD-FRP: 0.18; AOD-LST: -0.02).

Temporal association between FRP-AOD and LST clearly illustrates the immediate response of fire-associated changes in aerosol loading and surface temperature over the northwest part of India. In the subsequent section, such association was therefore, modelled using a geospatial tree-based regression model using several concurrent temporal (like day-specific retrieval) and spatial features (like regional meteorology, aerosol loading and fire intensity) to construct FRP-AOD-LST nexus over intensive fire zone in northwest India.

3.4 Fire induced change in LST and AOD

Crop-residue based fire induced change in surface temperature and aerosol loading was quantified using space-for-time approach, overlaying grid-based VIIRS LST, FRP and AOD at 10x10 km^2 resolution over year-specific intensive fire zone. As illustrated in Fig. 7, with year-specific dataset included in Table S4, a clear and robust pattern of change in LST and AOD was noted over the areas exhibiting residue-based fire against that of no fire zone. Results are reported in terms of anomaly where a positive (negative) ΔLST indicates reginal warming (cooling). Fire induced an increase in LST by 0.48 °C over the fire zone during year 2017 to 2021, with marked temporal heterogeneity in temperature change with a range varying from -0.55 to 1.69 °C. It imply that there was instance when fire had cooling effect on surface temperature, as was in year 2019, although a very limited number of grid (2) exhibiting no fire could possibly the reason behind such unanticipated result. Barring this, an increase in LST was accounted in each year averaging 0.72 °C $year^{-1}$ which could possibly due to reduced evapotranspiration, as was also noted during forest fire (Liu et al., 2018, 2019).

https://doi.org/10.5194/egusphere-2025-3163
Preprint. Discussion started: 15 August 2025

Similarly, Zhang et al. (2020) asserted an increase in LST by 1-3 °C by agriculture residue-based fire in three provinces across China.

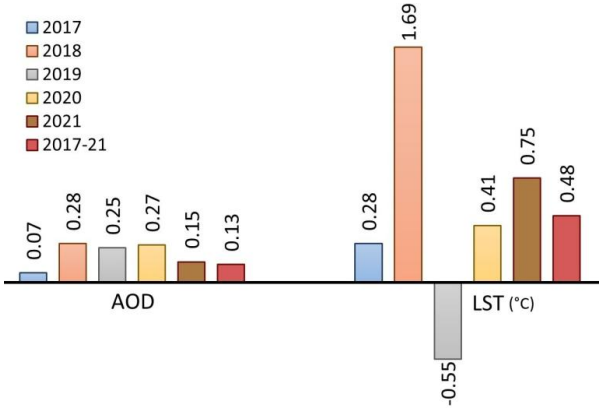

Fig. 7. Crop-residue based fire induced change in LST and AOD over intensive fire zone.

A consistent increase in aerosol loading was also accounted over the grids encountered with fire against no fire zone. Satellite based observation shows a clear trend in increasing AOD over the fire zone with a mean rise of 0.19 AOD year^{-1} with a range 0.07 to 0.28 AOD year^{-1}. Interestingly, increase in AOD was consistent across the monitoring period which link biomass burning emission with elevated aerosol emission over the source region, reported in literature across the globe (Mhawish et al., 2022; Ravindra et al., 2023).

3.5 Spatial regression of fire intensity and aerosols on LST

To establish a possible association between predictors *viz*. fire intensity, aerosols and meteorology on dependent variable LST, a machine learning algorithm was employed hypothesizing non-linear statistical association among the variables. The choice of Random Forest (RF) to regress the association was based on its excellent accuracy, ability to handle large dataset, superior performance and prior applications on LST-based research (Logan et al., 2020; Wang et al., 2022; Zhang et al., 2025). Here, relative importance of fire intensity, aerosol loading and meteorological variables (Fig. S5) were assessed to sustain spatial variations in LST across the year-constrained intensive fire zone. Further, relative contributions of each predictors were quantified and marginal effects of predictor variables on LST have been quantified. Two pre-specified scenarios (Table S5), one, that includes days with extended fire intensity starting from fire initiation to terminate, and second, days including high intensity fire having strong positive correlation between FRP and LST were

https://doi.org/10.5194/egusphere-2025-3163
Preprint. Discussion started: 15 August 2025

modelled. Such approximation were meant to evaluate and compare the relative importance of predictor variables both in the cases of high intensity fire and during entire crop-based fire episode.

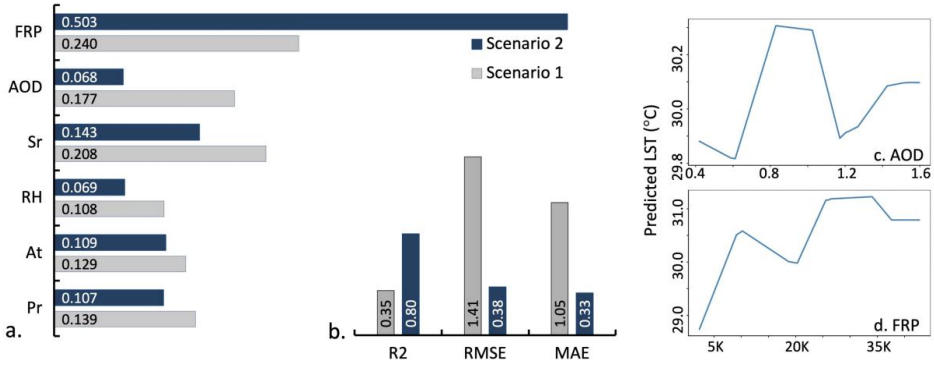

Fig. 8. Relative feature importance of predictor variables on LST (a), statistical performance of random forest for two diverse scenarios (b), and partial dependence plots of LST on AOD (c) and FRP (d).

NOTE. For Fig. 8d, K indicates x1000. The PDP plots are based on scenario 2.

Figure 8(a) indicate the relative feature importance (RFI) of the selected predictor variables modelled across the identified scenarios. Variable relative feature importance refers the sensitivity of LST against individual predictors and serves as an identity about their partial influence in predicting LST. Scenario 1 resulted the strongest influence of FRP (RFI: 0.240) on LST across the intensive fire zone followed by solar radiation (0.208) and aerosol loading (0.177). The partial influence of other parameters including meteorological variables were less significant (<0.140). The prediction of FRP as the top feature to modulate LST changes during crop residue-based fire event is imperative as it hold greater repercussion on the regional climate and human health. However, the RFI scores for both FRP and SR were comparable indicating their shared partial influence on LST. Another interesting finding was to attain significant impact of columnar aerosol loading on LST modification which was otherwise reported by researchers investigating global fire aerosols and climate (Tian et al., 2022). It is noteworthy that RF model performance for the scenario 1 records high RMSE (1.41) and MAE (1.05) with comparatively low R^2 (0.35) which translates into some uncertainties in the prediction.

https://doi.org/10.5194/egusphere-2025-3163
Preprint. Discussion started: 15 August 2025

In contrast, a superior model performance was achieved in case of scenario 2 when very high coefficient of determination (R^2: 0.80) was accounted with sufficiently less RMSE (0.38) and MAE (0.33). This ensured a robust model prediction when high correlation coefficient between FRP and LST were selectively considered. Interestingly, FRP also emerged as the top feature in modulating LST variation during scenario 2 with robust RFI of 0.503. This essentially establish the added contribution of excessive heat energy released during high intensity fire on LST modifications over high intensity residue-based fire zone. The very next contribution on LST variations was due to SR (RFI: 0.143) and aerosol loading (RFI: 0.68) which emerged to reduce significantly against scenario 1 when fire intensity spread across over extended time period. The partial dependence plot (PDP) on the marginal effects of FRP and AOD on LST have been included in Fig. 8(c-d). This indicates the relative change in LST with corresponding unit change in predictor variable when other predictors remain stable. The effect estimates of unit increase in AOD on LST remained inconsistent because of sudden reversal of trend when AOD remain within 1.00 to 1.20. In contrast, the marginal effect of FRP on LST has been prominent with an increase in regional FRP resulted in consequent increase in LST for almost all the cases. The RF model therefore, concludes with certainty the implications of crop-residue based fire associated release of energy and aerosols on regional LST which could have diverse consequences on regional climate, agriculture and human health.

3.6 Geographically weighted regression on LST

Initially, Global Moran' I test was performed to verify spatial autocorrelation in LST across the intensive fire zone cumulatively for five years. Results, as in Table S6, indicate Moran'I value (0.224) for LST has a high positive Z-score and remain spatially significant (p-value: 0.000). This refers very less possibility (<1%) of the clustered LST pattern could be due to random chance. Therefore, geographically weighted regression (GWR) was performed to assess spatial heterogeneity in FRP driven variations on LST across year-specific intensive fire zone over northwest India. GWR was however, simulated only for the main predictor FRP against dependent LST for scenario 2 based on prior outcome from RF regression. Figure 9 details the spatial outcome of GWR for the entire duration while model running criteria and year-wise performance is included in Table S7. Results indicate spatial heterogeneity in coefficient estimates with overall positive values over the intensive fire zone. It was however,

https://doi.org/10.5194/egusphere-2025-3163
Preprint. Discussion started: 15 August 2025

predictable as FRP over the intensive fire zone did vary with time and space which potentially influence LST at a diverse scale. Overall, GWR model clearly imply that higher FRP is primarily associated with increase in LST over the region which potentially have implications on regional climate and agriculture.

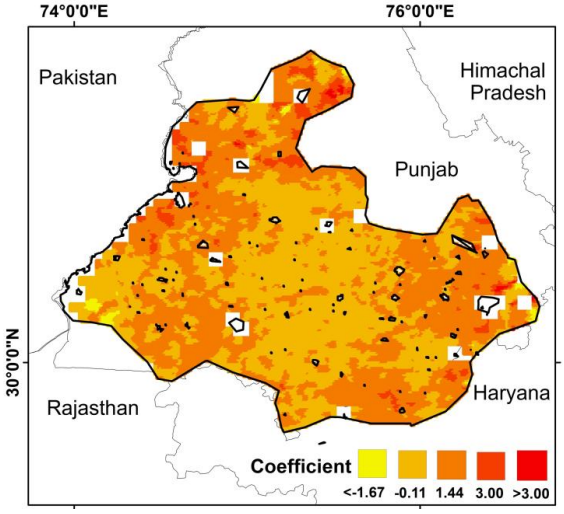

Fig. 9. Spatial distribution of GWR coefficients across intensive fire zone.

Conclusions

This analysis reveals that physical effect of crop-residue based fire can substantially affect the regional climate by modifying land surface temperature over an extensive geographical region in northwest India. However, the magnitude of surface temperature modification could vary with intensity of fire and associated modulation by regional meteorology. Results reported here were in line with the findings of Liu et al. (2019) when satellite-based observations on forest fire was held accountable for 0.15 K rise in surface temperature over burned area globally, and a net warming over Siberian Boreal Forest (Liu et al. (2018). There are other evidences too, as in Alkama and Cascatti (2016), Zhao et al. (2024) when incidences and intensities of forest fire were positively linked with temperature. However, biophysical effects of agriculture residue-based fire on land surface temperature are observationally scarce, making it difficult to constrain its environmental consequences over diverse landforms. In a recent work, Zhang et al. (2020) has found association of elevated land surface temperature over three different provinces in China due to crop residual burning. However, feedback of air temperature on fire incidences were not included for consideration.

https://doi.org/10.5194/egusphere-2025-3163
Preprint. Discussion started: 15 August 2025

Our effort in understanding residue-based fire associated changes in surface temperature was therefore, novel considering the extensive and recurrent fire incidences over northern India that has been associated with deteriorating air quality in Delhi and its surroundings. The findings of this study are however, limited with inability to measure counter feedback of the agriculture system towards limiting changes in land surface temperature, uncertainty associated with estimating fire radiative power, and accounting aerosols counter feedback on local meteorology and vice-versa.

The manuscript unfolds with identifying geospatial variations in crop residue-based fire, associated aerosol loading and land surface temperature over northern part of India. Based on year wise pixel-based fire intensity, geographical region encompassing intensive fire was earmarked and all satellite-based retrievals and reanalysis datasets were processed only over the selected zone. A robust spatial variation in FRP matched well with corresponding AOD and LST, providing first evidence on possible perturbations of fire on land surface temperature. Hurst exponent reaffirms long-term persistence of fire intensity, surface temperature and aerosol loading time-series. Spatial correlation established a strong temporal association between predictor and dependent variables that too constrained with years. A grid-based analysis over the intensive fire zone concluded a robust increase in LST and AOD during peak fire season.

The article further introduces Random Forest model and Geographically Weighted Regression to ascertain the potential influence of FRP and aerosol loading on LST, taking into account the existing meteorological variables over the selected zone. Two contrasting scenarios were hypothesized to regress the FRP-LST-AOD nexus. Scenario one, considered spatially aggregate FRP from fire initiating days to subside while scenario two accounted for days with very high intensity fire with strong and positive correlation between FRP and LST. Interestingly, for both the cases RF regression was able to capture and map the FRP induced modulation in LST with varying intensities and model performance. A clear increment in FRP induced LST modulation was noted especially during high intensity fire events. Beside FRP, both solar radiation and columnar aerosol loading also noted to partially influence the LST variations although with different intensities. However, the influence of columnar aerosol loading on LST seems to enhance during days with intense energy release possibly linked to excessive emission of carbonaceous aerosols from biomass burning. As Global Moran' I test

https://doi.org/10.5194/egusphere-2025-3163
Preprint. Discussion started: 15 August 2025

concludes significant clustering in LST over the intensive fire zone, the interrelationship between LST and FRP were further assessed using geographically weighted regression. GWR output put further evidences on FRP modulated LST variations over northwest India although it appears to vary strongly with respect to space. Our study therefore, provides a comprehensive insight into the distinctive and persistent LST responses to fire intensity, emphasizing the importance of recognizing the climate feedback from crop residue-based fire dynamics.

Acknowledgments

Authors acknowledges the fund received from Climate Change Programme, Department of Science and Technology (DST/CCP/CoE/80/2017-G) and Banaras Hindu University under Institute of Eminence grant (6031). Authors also acknowledge open source software like R (V4.4), Python (V3.7) and QGIS (V3.28) for extracting and plotting the dataset.

Data Availability

All the data used in this analysis are available freely. VIIRS and MODIS data can be accessed via NASA Earthdata (https://earthdata.nasa.gov) (last accessed: May 30, 2025), and AgERA5 reanalysis data is available from ECMWF Copernicus (https://cds.climate.copernicus.eu/) (last accessed: May 30, 2025). We thank NASA for providing the VIIRS and MODIS data, and the Copernicus Climate Change Service (C3S) for the AgERA5 reanalysis data.

Authors contributions

AP: Data curation, formal analysis and interpretation; RS: Data curation, formal analysis; KA: Data curation, formal analysis; NC: Data curation, formal analysis; TB: conceptualization, methodology and interpretation, funding as well as writing and editing manuscript.

Competing interests. Authors declare that they have no conflict of interest.

Supporting Information. The supporting tables (7) and figures (5) are included in supplementary file.

Bibliography

Aditi, K., Pandey, A. and Banerjee, T., 2025. Forest fire emission estimates over South Asia using Suomi-NPP VIIRS-based thermal anomalies and emission inventory. Environmental Pollution, 366, p.125441.

https://doi.org/10.5194/egusphere-2025-3163
Preprint. Discussion started: 15 August 2025

Aditi, K., Singh, A. and Banerjee, T., 2023. Retrieval uncertainty and consistency of Suomi-NPP VIIRS Deep Blue and Dark Target aerosol products under diverse aerosol loading scenarios over South Asia. Environmental Pollution, 331, p.121913.

Alkama, R. and Cescatti, A., 2016. Biophysical climate impacts of recent changes in global forest cover. Science, 351(6273), pp.600-604.

Andela, N., Morton, D.C., Giglio, L., Chen, Y., van der Werf, G.R., Kasibhatla, P.S., DeFries, R.S., Collatz, G.J., Hantson, S., Kloster, S. and Bachelet, D., 2017. A human-driven decline in global burned area. *Science*, *356*(6345), pp.1356-1362.

Balwinder-Singh, McDonald, A.J., Srivastava, A.K. *et al.* Tradeoffs between groundwater conservation and air pollution from agricultural fires in northwest India. *Nat Sustain* **2**, 580–583 (2019). https://doi.org/10.1038/s41893-019-0304-4.

Banerjee, T., Anchule, A., Sorek-Hamer, M. and Latif, M.T., 2022. Vertical stratification of aerosols over South Asian cities. Environmental Pollution, 309, p.119776.

Banerjee, T., Shitole, A.S., Mhawish, A., Anand, A., Ranjan, R., Khan, M.F., Srithawirat, T., Latif, M.T. and Mall, R.K., 2021. Aerosol climatology over South and Southeast Asia: Aerosol types, vertical profile, and source fields. Journal of Geophysical Research: Atmospheres, 126(6), p.e2020JD033554.

Bond, T.C., Doherty, S.J., Fahey, D.W., Forster, P.M., Berntsen, T., De Angelo, B.J., et al., 2013. Bounding the role of black carbon in the climate system: a scientific assessment. J. Geophys. Res. 118, 5380e5552.

Bowman, D.M., Balch, J.K., Artaxo, P., Bond, W.J., Carlson, J.M., Cochrane, M.A., d'Antonio, C.M., DeFries, R.S., Doyle, J.C., Harrison, S.P. and Johnston, F.H., 2009. Fire in the Earth system. science, 324(5926), pp.481-484.

Breiman, L. (2001). Random forests. *Machine learning*, *45*, 5-32.

Brunsdon, C., Fotheringham, A.S., Charlton, M.E., 1996. Geographically weighted regression: a method for exploring spatial nonstationarity. Geogr. Anal. 28, 281–298.

Brunsdon, C., Fotheringham, S., & Charlton, M. (1998). Geographically weighted regression. Journal of the Royal Statistical Society: Series D (The Statistician), 47(3), 431-443.

Chen, J., Shao, Z., Huang, X., Zhuang, Q., Dang, C., Cai, B., Zheng, X. and Ding, Q., 2022. Assessing the impact of drought-land cover change on global vegetation greenness and productivity. *Science of the Total Environment*, *852*, p.158499.

Chuvieco, E., Pettinari, M.L., Koutsias, N., Forkel, M., Hantson, S. and Turco, M., 2021. Human and climate drivers of global biomass burning variability. *Science of the Total Environment*, *779*, p.146361.

https://doi.org/10.5194/egusphere-2025-3163
Preprint. Discussion started: 15 August 2025

Copernicus Climate Change Service (2020). Agrometeorological indicators from 1979 to present derived from reanalysis. Copernicus Climate Change Service (C3S) Climate Data Store (CDS). DOI: 10.24381/cds.6c68c9bb (Accessed on February 25, 2025).

Daoud, J. I. (2017, December). Multicollinearity and regression analysis. In *journal of physics: Conference series* (Vol. 949, No. 1, p. 012009). IOP Publishing.

Fotheringham, A. S., Brunsdon, C., & Charlton, M. (2009). Geographically weighted regression. The Sage handbook of spatial analysis, 1, 243-254.

Giglio, L., Descloitres, J., Justice, C. O., & Kaufman, Y. J. (2003). An enhanced contextual fire detection algorithm for MODIS. Remote Sensing of Environment, 87, 273–282.

Gomez, J.L., Allen, R.J. and Li, K.F., 2024. California wildfire smoke contributes to a positive atmospheric temperature anomaly over the western United States. Atmospheric Chemistry and Physics, 24(11), pp.6937-6963.

Graham, M. H. (2003). Confronting multicollinearity in ecological multiple regression. *Ecology*, *84*(11), 2809-2815.

Graham, M.H., Haynes, R.J. and Meyer, J.H., 2002. Soil organic matter content and quality: effects of fertilizer applications, burning and trash retention on a long-term sugarcane experiment in South Africa. *Soil biology and biochemistry*, *34*(1), pp.93-102.

Hurst, H., 1951. Long term storage capacity of reservoirs. Trans. Am. Soc. Civil Eng. 6, 770–799.

Hsu, N.C., Herman, J.R. and Tsay, S.C., 2003. Radiative impacts from biomass burning in the presence of clouds during boreal spring in southeast Asia. Geophysical Research Letters, 30(5).

Ichoku, C., Giglio, L., Wooster, M.J. and Remer, L.A., 2008. Global characterization of biomass-burning patterns using satellite measurements of fire radiative energy. *Remote sensing of Environment*, *112*(6), pp.2950-2962.

Jethva, H., Torres, O., Field, R. D., Lyapustin, A., Gautam, R., & Kayetha, V. (2019). Connecting crop productivity, residue fires, and air quality over northern India. *Scientific Reports*, 9(1), 16594.

Kant, S., Sarangi, C. and Wilcox, E.M., 2023. Aerosol processes perturb cloud trends over Bay of Bengal: observational evidence. *npj Climate and Atmospheric Science*, *6*(1), p.132.

Korontzi, S., McCarty, J., Loboda, T., Kumar, S. and Justice, C.. (2006). Global distribution of agricultural fires in croplands from 3 years of Moderate Resolution Imaging Spectroradiometer (MODIS) data. Global Biogeochemical Cycles, 20(2).

Lasko, K. and Vadrevu, K., 2018. Improved rice residue burning emissions estimates: Accounting for practice-specific emission factors in air pollution assessments of Vietnam. *Environmental pollution*, *236*, pp.795-806.

https://doi.org/10.5194/egusphere-2025-3163
Preprint. Discussion started: 15 August 2025

Li, F., Zhang, X., Kondragunta, S., Csiszar, I., 2018. Comparison of fire radiative power estimates from VIIRS and MODIS observations. J. Geophys. Res. Atmos. 123 (9), 4545–4563.

Li, Z.L., Wu, H., Duan, S.B., Zhao, W., Ren, H., Liu, X., Leng, P., Tang, R., Ye, X., Zhu, J. and Sun, Y., 2023. Satellite remote sensing of global land surface temperature: Definition, methods, products, and applications. *Reviews of Geophysics*, *61*(1).

Liu, Z., Ballantyne, A. P., & Cooper, L. A. (2018). Increases in land surface temperature in response to fire in Siberian boreal forests and their attribution to biophysical processes. Geophysical Research Letters, 45, 6485–6494. https://doi.org/10.1029/2018GL078283.

Liu, Z., Ballantyne, A.P. and Cooper, L.A., 2019. Biophysical feedback of global forest fires on surface temperature. *Nature communications*, *10*(1), p.214.

Logan, T. M., Zaitchik, B., Guikema, S., & Nisbet, A. (2020). Night and day: The influence and relative importance of urban characteristics on remotely sensed land surface temperature. Remote Sensing of Environment, 247, Article 111861.

Lan, R., Eastham, S.D., Liu, T., Norford, L.K. and Barrett, S.R., 2022. Air quality impacts of crop residue burning in India and mitigation alternatives. Nature communications, 13(1), p.6537.

Markonis, Y., Koutsoyiannis, D., 2016. Scale-dependence of persistence in precipitation records. Nat. Clim. Chang. 6, 399–401. https://doi.org/10.1038/nclimate2894.

Mhawish, A., Sarangi, C., Babu, P., Kumar, M., Bilal, M. and Qiu, Z., 2022. Observational evidence of elevated smoke layers during crop residue burning season over Delhi: Potential implications on associated heterogeneous PM2. 5 enhancements. *Remote Sensing of Environment*, *280*, p.113167.

Markonis, Y., Koutsoyiannis, D., 2016. Scale-dependence of persistence in precipitation records. Nat. Clim. Chang. 6, 399–401. https://doi.org/10.1038/nclimate2894

Nguyen, H.M. and Wooster, M.J., 2020. Advances in the estimation of high Spatio-temporal resolution pan-African top-down biomass burning emissions made using geostationary fire radiative power (FRP) and MAIAC aerosol optical depth (AOD) data. *Remote Sensing of Environment*, *248*, p.111971.

Prasad, V.K., Gupta, P.K., Sharma, C., Sarkar, A.K., Kant, Y., Badarinath, K.V.S., Rajagopal, T. and Mitra, A.P., 2000. NOx emissions from biomass burning of shifting cultivation areas from tropical deciduous forests of India–estimates from ground-based measurements. *Atmospheric Environment*, *34*(20), pp.3271-3280.

Peng, J., Liu, Z., Liu, Y., Wu, J. and Han, Y., 2012. Trend analysis of vegetation dynamics in Qinghai–Tibet Plateau using Hurst Exponent. Ecological Indicators, 14(1), pp.28-39.

Puissant, A., Rougier, S., & Stumpf, A. (2014). Object-oriented mapping of urban trees using Random Forest classifiers. *International Journal of Applied Earth Observation and Geoinformation*, *26*, 235-245.

https://doi.org/10.5194/egusphere-2025-3163
Preprint. Discussion started: 15 August 2025

Ravindra, K., Singh, T., Singh, V., Chintalapati, S., Beig, G. and Mor, S., 2023. Understanding the influence of summer biomass burning on air quality in North India: Eight cities field campaign study. *Science of The Total Environment*, *861*, p.160361.

Granero, M.S., Segovia, J.T. and Pérez, J.G., 2008. Some comments on Hurst exponent and the long memory processes on capital markets. Physica A: Statistical Mechanics and its applications, 387(22), pp.5543-5551.

Sarkar, S., Singh, R.P. and Chauhan, A., 2018. Crop residue burning in northern India: Increasing threat to Greater India. *Journal of Geophysical Research: Atmospheres*, *123*(13), pp.6920-6934.

Sayer, A.M., Hsu, N.C., Lee, J., Kim, W.V., Dutcher, S.T., 2019. Validation, stability, and consistency of MODIS collection 6.1 and VIIRS version 1 deep blue aerosol data over land. J. Geophys. Res. Atmos. 124, 4658–4688

Schroeder, W., Oliva, P., Giglio, L. and Csiszar, I.A., 2014. The New VIIRS 375 m active fire detection data product: Algorithm description and initial assessment. *Remote Sensing of Environment*, *143*, pp.85-96.

Shyamsundar, P., Springer, N.P., Tallis, H., Polasky, S., Jat, M.L., Sidhu, H.S., Krishnapriya, P.P., Skiba, N., Ginn, W., Ahuja, V. and Cummins, J., 2019. Fields on fire: Alternatives to crop residue burning in India. *Science*, *365*(6453), pp.536-538.

Singh, N., Banerjee, T., Raju, M.P., Deboudt, K., Sorek-Hamer, M., Singh, R.S. and Mall, R.K., 2018. Aerosol chemistry, transport, and climatic implications during extreme biomass burning emissions over the Indo-Gangetic Plain. *Atmospheric Chemistry and Physics*, *18*(19), pp.14197-14215.

Singh, P., Roy, A., Bhasin, D., Kapoor, M., Ravi, S. and Dey, S., 2021. Crop fires and cardiovascular health–a study from North India. *SSM-Population Health*, *14*, p.100757.

Singh, T., Biswal, A., Mor, S., Ravindra, K., Singh, V. and Mor, S., 2020. A high-resolution emission inventory of air pollutants from primary crop residue burning over Northern India based on VIIRS thermal anomalies. *Environmental Pollution*, *266*, p.115132.

Singh, T., Ravindra, K., Beig, G. and Mor, S., 2021. Influence of agricultural activities on atmospheric pollution during post-monsoon harvesting seasons at a rural location of Indo-Gangetic Plain. *Science of The Total Environment*, *796*, p.148903.

Singh, T., Ravindra, K., Sreekanth, V., Gupta, P., Sembhi, H., Tripathi, S.N., Mor, S., 2020. Climatological trends in satellite-derived aerosol optical depth over North India and its relationship with crop residue burning: Rural-urban contrast. Sci. Total Environ. https://doi.org/10.1016/j.scitotenv.2020.140963.

Streets, D.G., Yarber, K.F.,Woo, J.H., Carmichael, G.R., 2003. Biomass burning in Asia: annual and seasonal estimates and atmospheric emissions. Global Biogeochem. Cycles 17.

https://doi.org/10.5194/egusphere-2025-3163
Preprint. Discussion started: 15 August 2025

Tian, C., Yue, X., Zhu, J., Liao, H., Yang, Y., Lei, Y., Zhou, X., Zhou, H., Ma, Y. and Cao, Y., 2022. Fire–climate interactions through the aerosol radiative effect in a global chemistry–climate–vegetation model. Atmospheric Chemistry and Physics, 22(18), pp.12353-12366.

Vadrevu, K. and Lasko, K., 2018. Intercomparison of MODIS AQUA and VIIRS I-Band fires and emissions in an agricultural landscape—Implications for air pollution research. *Remote Sensing*, *10*(7), p.978.

Vinjamuri, K.S., Mhawish, A., Banerjee, T., Sorek-Hamer, M., Broday, D.M., Mall, R.K. and Latif, M.T., 2020. Vertical distribution of smoke aerosols over upper Indo-Gangetic Plain. Environmental pollution, 257, p.113377.

van Der Velde, I.R., Van Der Werf, G.R., Houweling, S., Eskes, H.J., Veefkind, J.P., Borsdorff, T. and Aben, I., 2020. Biomass burning combustion efficiency observed from space using measurements of CO and NO 2 by TROPOMI. Atmospheric Chemistry and Physics Discussions, 2020, pp.1-65.

Wan, Z. (2014). New refinements and validation of the collection-6 MODIS land-surface temperature/emissivity product. Remote Sensing of Environment, 140, 36–45. https://doi.org/10.1016/j.rse.2013.08.027

Ward, D.S., Kloster, S., Mahowald, N.M., Rogers, B.M., Randerson, J.T. and Hess, P.G., 2012. The changing radiative forcing of fires: global model estimates for past, present and future. *Atmospheric Chemistry and Physics*, *12*(22), pp.10857-10886.

Wang, Q., Wang, X., Zhou, Y., Liu, D. and Wang, H., 2022. The dominant factors and influence of urban characteristics on land surface temperature using random forest algorithm. Sustainable Cities and Society, 79, p.103722.

Wooster, M.J., Roberts, G., Perry, G.L.W. and Kaufman, Y.J., 2005. Retrieval of biomass combustion rates and totals from fire radiative power observations: FRP derivation and calibration relationships between biomass consumption and fire radiative energy release. *Journal of Geophysical Research: Atmospheres*, *110*(D24).

Wooster, M.J., Zhukov, B. and Oertel, D., 2003. Fire radiative energy for quantitative study of biomass burning: Derivation from the BIRD experimental satellite and comparison to MODIS fire products. *Remote Sensing of Environment*, *86*(1), pp.83-107.

Yang, Q., Yuan, Q., Yue, L., & Li, T. (2020). Investigation of the spatially varying relationships of PM2.5 with meteorology, topography, and emissions over China in 2015 by using modified geographically weighted regression. Environmental Pollution, 262(4), 114257.

Yin, S., 2020. Biomass burning spatiotemporal variations over South and Southeast Asia. *Environment International*, *145*, p.106153.

Zhang, Y., Ge, J., Bai, X. and Wang, S., 2025. Blue-Green space seasonal influence on land surface temperatures across different urban functional zones: Integrating Random Forest and geographically weighted regression. Journal of Environmental Management, 374, p.123975.

https://doi.org/10.5194/egusphere-2025-3163
Preprint. Discussion started: 15 August 2025

860 Zhang, W., Yu, M., He, Q., Wang, T., Lin, L., Cao, K., Huang, W., Fu, P. and Chen, J., 2020. The
861 spatial and temporal impact of agricultural crop residual burning on local land surface
862 temperature in three provinces across China from 2015 to 2017. Journal of Cleaner
863 Production, 275, p.124057.

864 Zhao, J., Yue, C., Wang, J., Hantson, S., Wang, X., He, B., Li, G., Wang, L., Zhao, H. and Luyssaert,
865 S., 2024. Forest fire size amplifies postfire land surface warming. Nature, 633(8031), pp.828-
866 834.

867